

RSC Advances



This is an *Accepted Manuscript*, which has been through the Royal Society of Chemistry peer review process and has been accepted for publication.

Accepted Manuscripts are published online shortly after acceptance, before technical editing, formatting and proof reading. Using this free service, authors can make their results available to the community, in citable form, before we publish the edited article. This *Accepted Manuscript* will be replaced by the edited, formatted and paginated article as soon as this is available.

You can find more information about *Accepted Manuscripts* in the [Information for Authors](#).

Please note that technical editing may introduce minor changes to the text and/or graphics, which may alter content. The journal's standard [Terms & Conditions](#) and the [Ethical guidelines](#) still apply. In no event shall the Royal Society of Chemistry be held responsible for any errors or omissions in this *Accepted Manuscript* or any consequences arising from the use of any information it contains.

COMMUNICATION

Photovoltaic Performance of Ladder-type Indacenodithieno[3,2-*b*]thiophene-Based Polymers with Alkoxyphenyl Side Chains

Cite this: DOI:
10.1039/x0xx00000x

Yue Zang,^{a,b} Yun-Xiang Xu,^{b,c} Chu-Chen Chueh,^b Chang-Zhi Li,^b Hsiu-Cheng Chen,^d Kung-Hwa Wei,^d Jun-Sheng Yu,^{a*} and Alex K.-Y. Jen^{b*}

Received 00th January 2012,
Accepted 00th January 2012

DOI: 10.1039/x0xx00000x

www.rsc.org/

Two new ladder-type conjugated polymers, PIDTT-DFBT-EH and PIDTT-F-PhanQ-EH, are prepared through the copolymerization of heptacyclic IDTT with F-PhanQ and DFBT electron deficient moieties. The introduction of 4-(2-ethylhexyloxy)-phenyl (EHOPh) side-chains onto polymer is beneficial for achieving high molecular weight and good solution-processability of materials. The derived polymer solar cells yielded PCEs of 5.48% (PIDTT-DFBT-EH) and 5.14% (PIDTT-F-PhanQ-EH), without engaging post-solvent or solvent additive treatments.

Introduction

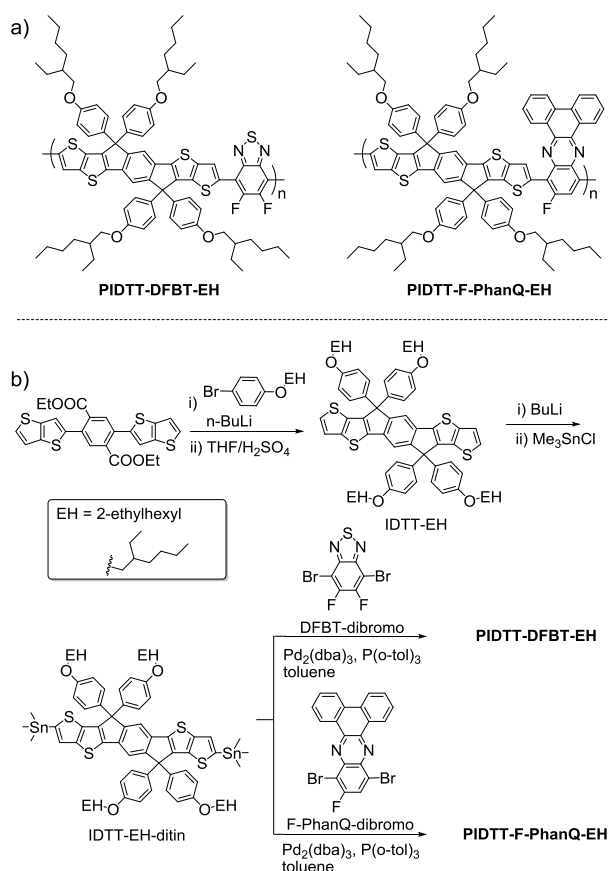
Polymer solar cells (PSCs) have attracted significant interests in the past decades. Thus far, the state-of-the-art power conversion efficiencies (PCEs) of PSCs have already reached >10% milestone in single bulk-heterojunction (BHJ) junction cells.¹⁻³ In general, solvent additives and special treatments (i.e solvent/thermal annealing) are needed for the majority of organic BHJs to obtain the optimal performance.⁴⁻⁵ The requirement of complicated processing might introduce variables and difficulties in translating these BHJs into high throughput manufacturing of PSCs. In this regard, some high-performance ladder-type polymers have attracted the attentions, such as polyindacenodithiophene (PIDT) derivatives, due to the ease of obtaining homogenous, morphologically stable BHJ thin-films.⁶⁻²³ For example, Cheng *et al.* have demonstrated a seven-ring ladder polymer with a PCE of up to ~7% by fusing a fluorene unit together with two thiophene units.¹⁹ Meanwhile, Jen *et al.* have demonstrated that the PCE of ladder-type polymer, PIDT-DFBT, can be increased from 6% to 7% by extending the constituent thiophene ring in the IDT moiety to thieno[3,2-*b*]thiophene (TT) fused-ring (PIDTT-DFBT).²⁴

In addition to polymer backbone, the attachment of side-chains is also important which not only can dictate polymer solubility, but also can influence its phase behavior.^{21, 22, 25} In our previous work, PIDTT-DFBT has shown limited solubility in aromatic solvents, i.e. chlorobenzene (CB), *o*-Dichlorobenzene (DCB), due to its tendency of strong aggregation. This prevents us from obtaining high molecular weight (MW) polymer, which eventually affects the polymer's electronic properties.²³ In this work, we examine the effect of flexible side-chains of IDTT-based polymers on influencing their photovoltaic performance.

Herein, we report two novel donor-acceptor (D-A) alternating copolymers, PIDTT-F-PhanQ-EH and PIDTT-DFBT-EH, which are co-polymerized from IDTT donor with fluorinated quinoxaline (F-PhanQ) and benzodithizole (DFBT) electron deficient units (**Scheme 1**). Four 4-(2-ethylhexoxy)-phenyl side-chains are introduced to the planar IDTT moiety. Our results showed that the newly synthesized polymers possess relatively higher MW, with narrower polydispersity (PDI) compared to that of the parent PIDTT-DFBT with 4-hexylphenyl side-chains. Finally, we show that PSCs derived from PIDTT-F-PhanQ-EH and PIDTT-DFBT-EH BHJ can yield decent PCEs of 5.48% and 5.14%, respectively, with high V_{oc} over 0.90 V without using post-solvent annealing or solvent additives.

Results and discussion

The chemical structures of PIDTT-F-PhanQ-EH and PIDTT-DFBT-EH and the synthetic routes for IDTT-EH are depicted in **Scheme 1**. The detailed synthetic conditions are described in the Experiment Section. The MW of these polymers are measured by gel permeation chromatography (GPC) using monodispersed polystyrene as the standard and THF as the eluent. The PIDTT-F-PhanQ-EH and PIDTT-DFBT-EH have the number average molecular weight (M_n) of 42.3 and 38.2 kDa, with a PDI of 1.61 and 1.52, respectively. As can be clearly seen, the MW of PIDTT-DFBT-EH (38.2 kDa) are much higher compared to that of the parent PIDTT-DFBT (24.0 kDa) with 4-hexylphenyl side chains.²⁴ The two new polymers with 4-(2-ethylhexoxy)-phenyl side-chains can be readily dissolved in common solvents, such as CB, DCB, and chloroform (CHCl₃).



Scheme 1. (a) Chemical structures and (b) synthetic routes of PIDT-DFBT-EH and PIDTT-F-PhanQ-EH.

UV-Vis absorption spectra of the studied polymers in CHCl_3 solutions and in thin-films are shown in **Figure 1** and the relevant parameters are summarized in **Table 1**. Both polymers exhibited two characteristic absorption bands in the spectra. The band in short wavelength (~ 430 nm) is attributed to the π - π^* transition of the heptacyclic IDTT units, while the band at visible region (~ 640 nm) stems from the intramolecular charge transfer (ICT) between IDTT and electron deficient units. PIDTT-DFBT-EH polymer exhibits a relatively sharp and intense ICT peak compared to that of PIDTT-F-PhanQ-EH because DFBT is a stronger acceptor and smaller in size than F-PhanQ, which results in better ICT and backbone co-planarity. Note that the relative intensities of the ICT peak to the high energy peaks decreased in thin-film state than those in solution for both polymers. Our previous studies showed that ladder-type IDT and IDTT donor based polymers with 4-hexylphenyl side-chains are in general less-crystalline materials. It suggests that polymer chain-to-chain packing and backbone co-planarity might be disturbed when polymers are condensed from solution to thin-film state. The estimated optical bandgap of PIDTT-F-PhanQ-EH and PIDTT-DFBT-EH from the absorption band edges are 1.67 eV and 1.79 eV, respectively.

The electrochemical properties of these two polymers are investigated by cyclic voltammetry. Both polymers showed stable and reversible oxidation/reduction peaks in the cathodic and anodic scans (**Figure 2**). The redox potentials are measured against Ag/Ag^+ as the reference electrode with a platinum wire as the work electrode

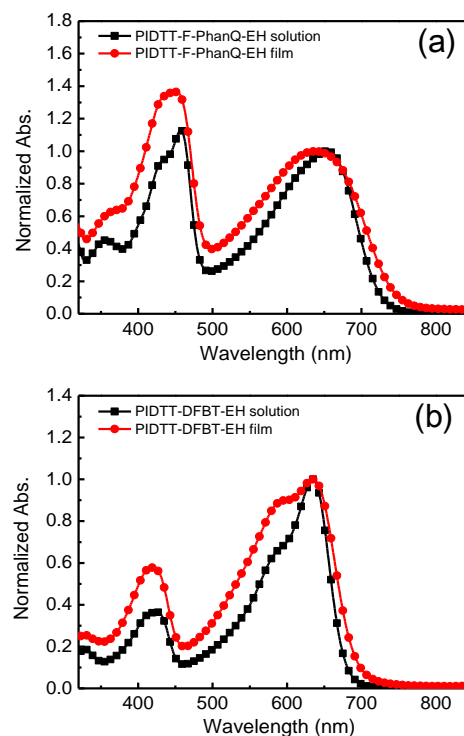


Figure 1. UV-vis spectra of (a) PIDTT-F-PhanQ-EH and (b) PIDTT-DFBT-EH in CHCl_3 solution and in thin-film state.

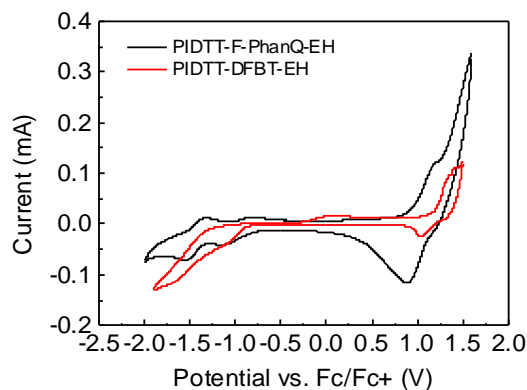


Figure 2. The CV curves of PIDTT-F-PhanQ-EH and PIDTT-DFBT-EH film.

and a platinum disc as the counter electrode in a 0.1 mol/L tetrabutylammoniumhexafluoro phosphate in acetonitrile with a scan rate of 100 mV s^{-1} . The highest occupied and lowest unoccupied molecular orbitals (HOMO and LUMO) of two polymers are calculated by the onset of the redox potentials (corrected with ferrocene standard). The HOMO levels for PIDTT-F-PhanQ-EH and PIDTT-DFBT-EH are -5.32 eV and -5.53 eV, respectively. These values are in an ideal range to assure good air-stability of polymers and large V_{OC} of the derived devices. The LUMO levels for PIDTT-F-PhanQ-EH and IDTT-DFBT-EH are -3.62 eV and -3.52 eV, respectively, which are positioned more than 0.3 eV above the LUMO of PC_{71}BM (4.1 eV). The estimated electrochemical

bandgaps of both polymers match well with the measured optical bandgaps.

PCE of 5.14% with a V_{OC} of 0.90 V, a J_{SC} of 10.31 mA cm⁻², and a FF of 0.55. The slightly lower V_{OC} of PIDTT-F-PhanQ-EH than

Table 1. Optical and electrochemical properties of studied polymers.

	M_n (kD _a)	PDI	λ_{max}^{soln} (nm)	λ_{max}^{film} (nm)	E_g^{opt} (eV)	HOMO (eV)	LUMO (eV)	E_g^{ec} (eV)
PIDTT-F-PhanQ-EH	42.3	1.61	652	636	1.67	-3.62	-5.32	1.70
PIDTT-DFBT-EH	38.2	1.52	635	635	1.79	-3.52	-5.53	2.01

High charge carrier mobilities of polymers are crucial for serving as efficient materials in PSCs. To evaluate charge mobility of the studied polymers, bottom gate and top-contact organic field-effect transistors (OFET) are conducted. Both polymers exhibited ambipolar charge-transporting behavior. The estimated hole- and electron-mobilities ($\mu_{sat,h}$ and $\mu_{sat,e}$) for PIDTT-F-PhanQ-EH are 3.80×10^{-3} and 2.70×10^{-3} cm² V⁻¹ s⁻¹, and for PIDTT-DFBT-EH are 9.20×10^{-4} and 5.40×10^{-3} cm² V⁻¹ s⁻¹, respectively.

To evaluate the photovoltaic performance of these polymers, a conventional configuration of ITO/PEDOT:PSS/polymer:PC₇₁BM (1:3)/Bis-C₆₀/Ag was primarily investigated.²⁶⁻²⁷ **Figure 3(a)** shows the J - V curves of the studied devices and the relevant parameters are summarized in **Table 2**. The devices based on PIDTT-DFBT-EH:PC₇₁BM BHJ exhibited a PCE of 5.48% with a V_{OC} of 0.95 V, a short current density (J_{SC}) of 11.16 mA cm⁻², and a fill factor (FF) of 0.52 while the PIDTT-F-PhanQ-EH based devices showed a lower

PIDTT-DFBT-EH can be attributed to the up-shifted HOMO level as abovementioned. To verify the change of J_{SC} , the external quantum efficiencies (EQEs) of the studied devices are measured and shown in **Figure 3(b)**. The J_{SC} values calculated from the EQE curves under the standard AM 1.5G conditions match well with the values obtained from J - V measurements. Note that all the BHJ blends are fabricated by simple spin-coating and annealed at 110 °C without using any post-solvent annealing or solvent additives. Comparing with the parent PIDTT-DFBT polymer, new polymers bearing 2-alkoxyphenyl side chains exhibit better processability. Whereas the charge mobilities are one to two-orders of magnitude lower than that of parent polymer. The decreased charge mobilities of new polymer would be responsible to the observed relatively low J_{sc} and FF for PIDTT-DFBT-EH and PIDTT-F-PhanQ-EH based devices.

Table 2. Photovoltaic characteristics of PIDTT-F-PhanQ-EH and PIDTT-DFBT-EH.

	V_{OC} (V)	J_{SC} (mA cm ⁻²)	FF	PCE (%)
PIDTT-F-PhanQ-EH	0.90	10.31	0.55	5.14
PIDTT-DFBT-EH	0.95	11.16	0.52	5.48

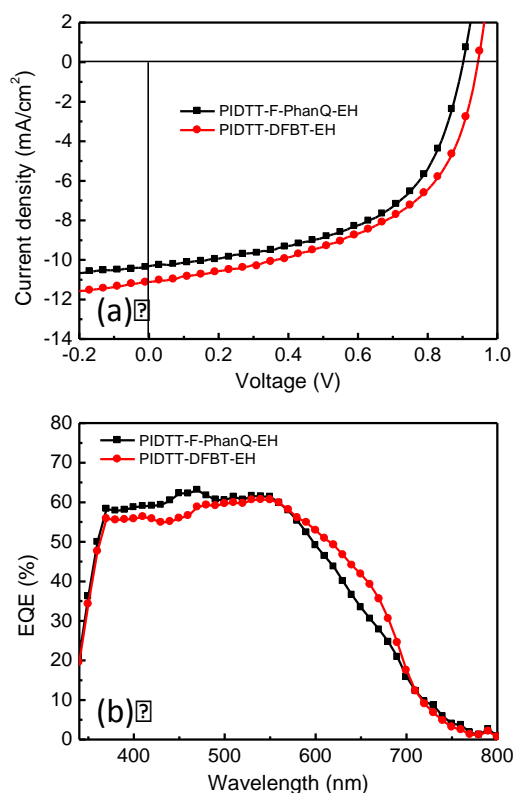


Figure 3. (a) Characteristic J - V curves and (b) EQE spectra for the BHJ solar cells derived from PIDTT-F-PhanQ-EH and PIDTT-DFBT-EH BHJ.

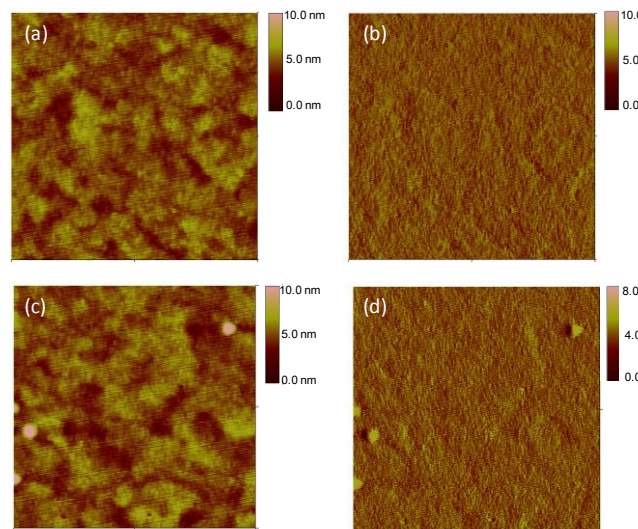


Figure 4. AFM height images (a,c) and phase images (b,d) of PIDTT-F-PhanQ-EH:PC₇₁BM (a,b) and PIDTT-DFBT-EH:PC₇₁BM (c,d) BHJ films.

In addition, similar thin film morphologies are observed in atomic force microscopy (AFM) measurements of two polymers blends (Figure 4). Smooth surface morphology of blends is obtained with a root-mean-square (RMS) roughness of 0.87 nm for PIDTT-F-PhanQ-EH and 1.02 nm for PIDTT-

DFBT-EH. As a result, PCEs of over 5% PCE are achieved in PIDTT-DFBT-EH-based devices through simple processing, which are quite appealing for applications in printed devices.

Conclusions

In summary, two novel ladder-type D-A copolymers PIDTT-F-PhanQ-EH and PIDTT-DFBT-EH are designed and synthesized with 4-(2-ethylhexoxy)-phenyl side-chains. The flexible side-chains enhance the solubility and processability of the resulting polymer as compared to the original polymer with 4-hexylphenyl side-chains. The PSCs made from PIDTT-DFBT-EH showed a PCE of 5.48%, and the device using PIDTT-F-PhanQ-EH showed a PCE of 5.14%. With regard to the simple processability of polymer blend induced by the incorporation of new side-chains, this represents an effective strategy in designing efficient wide band-gap materials that are adaptable for practical printing process of BHJ PSCs.

Experimental

Materials

All chemicals, unless otherwise specified, were purchased from Aldrich and used as received. DFBT-dibromo and F-PhanQ-dibromo were synthesized according to a previously reported procedure.²⁸

Synthesis of IDTT-EH

To a solution of 4-ethylhexyloxy-1-bromobenzene (2.20 g, 7.72 mmol) in THF (20 mL) at -78 °C was added n-BuLi (3.08 mL, 2.50 M), the mixture was kept at -78 °C for 1h, then a solution of compound 1 (800 mg, 1.6 mmol) in THF (20 mL) was added slowly. After the addition, the mixture was stirred at room temperature overnight and then poured into water and extracted twice with ethyl acetate. The combined organic phase was dried over Na₂SO₄. After removing the solvent, the crude product was charged into three-neck flask. Acetic acid (40 mL) and concentrated H₂SO₄ (0.8 mL) were added and the mixture was refluxed for 2h. Then the mixture was poured into water and extracted with ethyl acetate. The resulting crude compound was purified by silica gel column using a mixture of hexane/ DCM as the eluent to give a light yellow solid. ¹H NMR (500 MHz, CDCl₃, δ): 7.50 (s, 2 H), 7.30-7.27 (m, 4 H), 7.23 (d, *J* = 9.0 Hz, 8 H), 6.83 (d, *J* = 9.0 Hz, 8 H), 3.81 (d, *J* = 5.5 Hz, 8 H), 1.72-1.68 (m, 4 H), 1.53-1.31 (m, 32 H), 0.94-0.90 (m, 24 H); ¹³C NMR (125 MHz, CDCl₃, δ): 158.4, 153.6, 146.3, 142.9, 141.7, 135.9, 134.8, 133.6, 129.2, 126.3, 120.4, 116.6, 114.3, 70.2, 62.2, 39.4, 30.5, 29.0, 23.8, 23.0, 14.1, 11.1. MS (MALDI) *m/z*: [M]⁺ calcd for C₇₆H₉₀O₄S₄, 1194.572; found, 1194.721.

Synthesis of IDTT-EH-bis(trimethylstannane)

To a solution of IDTT-EH (321 mg, 0.27 mmol) in THF (10 mL) at -78 °C was added n-BuLi (0.30 mL, 0.74mmol, 2.5 M in hexane). After the addition, the mixture was kept at -78 °C for 1 h and then warmed to RT for another 30 min. After cooling back to -78 °C, trimethyltin chloride (0.81 mL, 1 M in hexane) was added dropwise. The resulting mixture was stirred overnight at RT, then poured into

water and extracted with hexane. After drying over Na₂SO₄, solvent was removed and ethanol was added. The precipitates were collected and dried as a solid. ¹H NMR (300 MHz, CDCl₃, δ): 7.42 (s, 2 H), 7.30 (s, 2 H), 7.19 (d, *J* = 8.7 Hz, 8 H), 6.79 (d, *J* = 8.7 Hz, 8 H), 3.78 (d, *J* = 5.7 Hz, 8 H), 1.69-1.64 (m, 4 H), 1.49-1.28 (m, 32 H), 0.91-0.85 (m, 24 H), 0.37 (s, 18 H). ¹³C NMR (125 MHz, CDCl₃, δ): . MS (MALDI) *m/z*: [M]⁺ calcd for C₈₂H₁₀₆O₄S₄Sn₂, 1520.5012; found, 1520.5006.

Polymerization of PIDTT-F-PhanQ-EH

IDTT-EH-di-Tin (130 mg, 0.085 mmol) and dibromo F-PhanQ (37 mg, 0.081 mmol) were charged in a 25 mL three-neck flask under argon. After adding toluene (3 mL), the mixture was degassed by three freeze/pump/thaw cycles to remove O₂. Then Pd₂(dba)₃ (3.9 mg, 5 mol%) and P(o-tol)₃ (10.3 mg, 0.034mmol) were added and the mixture was degassed once more. Then the mixture was heated at 120 °C for 3 days. After cooling to RT, the mixture was poured into methanol. The precipitate was collected and washed by Soxhlet extraction sequentially with acetone, hexane, and DCM. The remained solid in the filter was collected and dried (86 mg, 67%). ¹H NMR (300 MHz, CDCl₃, δ) 9.55-9.30 (m, 2 H), 8.34-8.18 (m, 1 H), 7.89-7.73 (m, 2 H), 7.69-7.60 (m, 2 H), 7.59-7.51 (m, 2 H), 7.52-7.29 (m, 10 H), 7.00-6.76 (m, 10 H), 4.02-3.55 (m, 8 H), 1.77-1.58 (m, 4 H), 1.47-1.32 (m, 8 H) 1.31-1.18 (m, 24 H), 0.97-0.76 (m, 24 H)

Polymerization of PIDTT-DFBT-EH

IDTT-EH-di-Tin (150 mg, 0.099 mmol) and dibromo DFBT (39.7 mg, 0.094 mmol) were charged in a 25 mL three-neck flask under argon. After adding toluene (3 mL), the mixture was degassed by three freeze/pump/thaw cycles to remove O₂. Then Pd₂(dba)₃ (4.5 mg, 5 mol%) and P(o-tol)₃ (12.1 mg, 0.040 mmol) were added and the mixture was degassed once more. Then the mixture was heated at 120 °C for 3 d. After cooling to RT, the mixture was poured into methanol. The precipitate was collected and washed by Soxhlet extraction sequentially with acetone, hexane, and DCM. The remained solid in the filter was collected and dried (97 mg, 72%). ¹H NMR. (300 MHz, CDCl₃, δ): 8.71-8.62 (m, 2 H), 7.59-7.49 (m, 2 H), 7.32-7.26 (m, 8 H), 6.91-6.78 (m, 8 H), 3.87-3.74 (m, 8 H), 1.71-1.65 (m, 4 H), 1.29 (m,32 H), 0.89 (t, *J* = 6.89 Hz, 24H).

General Characterization Methods

UV-Vis spectra were obtained using a Perkin-Elmer Lambda-9 spectrophotometer. The ¹H NMR spectra were collected on a Bruker AV 300 spectrometer operating at 300 MHz in d-chloroform solution with TMS as reference. MS spectra were recorded on Bruker Esquire LC-Ion Trap. Cyclic voltammetry of polymer films were measured against Ag/Ag⁺ as the reference electrode, ITO as working electrode and Pt mesh electrode in an 0.1 M electrolyte containing tetrabutylammoniumhexafluoro-phosphate in acetonitrile with a scan rate of 100 mV s⁻¹. The M_w was measured by a Waters 1515 gel permeation chromatograph with a refractive index detector at room temperature (THF as the eluent).

Fabrication of Polymer Solar Cells

ITO-coated glass substrates ($15 \Omega \text{ sq}^{-1}$) were cleaned with detergent, de-ionized water, acetone, and isopropyl alcohol. A thin layer (ca. 35 nm) of PEDOT:PSS (Baytron® P VP AI 4083, filtered at $0.45 \mu\text{m}$) was first spin-coated on the pre-cleaned ITO-coated glass substrates at 5,000 rpm and baked at 140°C for 10 minutes under ambient conditions. The substrates were then transferred into an argon-filled glove-box. Subsequently, the polymer:PC71BM active layer was spin-coated on the PEDOT:PSS layer at 1000 rpm from a homogeneously blended solution. The solution was prepared by dissolving the polymer and fullerene at weight ratios of 1:3 in dichlorobenzene to a total concentration of 20 mg/mL at 80°C overnight and filtered through a PTFE filter ($0.45 \mu\text{m}$). All of the substrates were placed on the hot plate at 110°C for 10 min. After annealing, a 10 nm thick film of C_{60} -bis surfactant (2 mg/mL in methanol) was spin-coated at 5000 rpm and then annealed at 110°C for 5 min to drive off any remaining solvent prior to metal deposition. At the final stage, the substrates were pumped down to high vacuum ($< 2 \times 10^{-6}$ Torr), and silver (100 nm) was thermally evaporated onto the active layer. Shadow masks were used to define the active area ($10.08 \times 10^{-2} \text{ cm}^2$) of the devices.

Characterization of Polymer Solar Cells

The current density-voltage (J - V) characteristics of unencapsulated photovoltaic devices were measured under N_2 using a Keithley 2400 source meter. A 300 W xenon arc solar simulator (Oriel) with an AM 1.5 global filter operated at 100 mW cm^{-2} was used to simulate the AM 1.5G solar irradiation. The illumination intensity was corrected by using a silicon photodiode with a protective KG5 filter calibrated by the National Renewable Energy Laboratory (NREL). The EQE system uses a lock-in amplifier (Stanford Research Systems SR830) to record the short circuit current under chopped monochromatic light.

Fabrication of Organic Field-Effect Transistors

Transistors were fabricated with top-contact and bottom-gate geometry. After cleaning the silicon substrate (with a 300 nm silicon oxide layer) by sequential ultrasonication in acetone and isopropyl alcohol for 15 min followed by air plasma treatment, the oxide layer was passivated with a thin divinyltetramethyldisiloxane-bis(benzocyclobutene) (BCB) buffer layer. The 1 wt% BCB precursor solution in toluene was spun onto the silicon oxide at 4000 rpm and subsequently annealed at 250°C overnight. The PIDTT-F-PhanQ-EH and PIDTT-DFBT-EH films were spin-coated from a 5 mg/mL DCB solution at 1000 rpm for 90 s. Interdigitated source and drain electrodes ($W=1000 \mu\text{m}$, $L=20/30/50 \mu\text{m}$) were defined by evaporating a Au (60 nm) through a shadow mask from the resistively heated Mo boat at 10^{-7} Torr.

Characterization of Organic Field-Effect Transistors

OFET characterization was carried out in a N_2 -filled glovebox using an Agilent 4155B semiconductor parameter S6 analyzer. The field-effect mobility was calculated in the saturation regime from the linear fit of $(I_{\text{ds}})^{1/2}$ vs V_{gs} . The threshold voltage (V_t) was estimated

as the x intercept of the linear section of the plot of $(I_{\text{ds}})^{1/2}$ vs V_{gs} . The sub threshold swing was calculated by taking the inverse of the slope of I_{ds} vs V_{gs} in the region of exponential current increase.

Acknowledgements

The authors thank the support from the Asian Office of Aerospace R&D (No. FA2386-11-1-4072), and the Office of Naval Research (No. N00014-14-1-0170). A. K.-Y. Jen thanks the Boeing Foundation for support. Y. Zang thanks the State-Sponsored Scholarship for Graduate Students from China Scholarship Council and Fundamental Research Funds for the Central Universities (No. ZYGX2012YB025). C.-C. Chueh thanks the final support from National Taiwan University (101R4000).

Notes and references

^aState Key Laboratory of Electronic Thin Films and Integrated Devices, School of Optoelectronic Information, University of Electronic Science and Technology of China (UESTC), Chengdu, 610054, P. R. China

^bDepartment of Materials Science and Engineering, University of Washington, Box 352120, Seattle, Washington, 98195, USA

^cCollege of Polymer Science and Engineering, State Key Laboratory of Polymer Materials and Engineering, Sichuan University, Chengdu, 610065, P. R. China

^dDepartment of Materials Science and Engineering, National Chiao Tung University, 300 Hsinchu, Taiwan

- G. Li, R. Zhu, Y. Yang, *Nat. Photon.* 2012, **6**, 153.
- C.-C. Chen, W.-H. Chang, K. Yoshimura, K. Ohya, J. You, J. Gao, Z. Hong, and Y. Yang, *Adv. Mater.* 2014, **26**, 5670.
- C.-Z. Li, C.-Y. Chang, Y. Zang, H.-X. Ju, C.-C. Chueh, P.-W. Liang, N. Cho, D. S. Ginger, and A. K.-Y. Jen, *Adv. Mater.* 2014, **26**, 6262.
- J. Zou, H.-L. Yip, Y. Zhang, Y. Gao, S.-C. Chien, K. O'Malley, C.-C. Chueh, H. Z. Chen, and A. K.-Y. Jen, *Adv. Funt. Mater.* 2012, **22**, 2840.
- C.-C. Chueh, K. Yao, H.-L. Yip, C.-Y. Chang, Y.-X. Xu, K.-S. Chen, C.-Z. Li, P. Liu, F. Huang, Y. W. Chen, W.-C. Chen, and A. K.-Y. Jen, *Energy Environ. Sci.* 2013, **6**, 3241.
- C.-Y. Yu, C.-P. Chen, S.-H. Chan, G.-W. Hwang, C. Ting, *Chem. Mater.* 2009, **21**, 3262.
- S.-H. Chan, C.-P. Chen, T.-C. Chao, C. Ting, C.-S. Lin, B.-T. Ko, *Macromolecules* 2008, **41**, 5519.
- C. P. Chen, S. H. Chan, T. C. Chao, C. Ting, B. T. Ko, *J. Am. Chem. Soc.* 2008, **130**, 12828.
- I. McCulloch, R. S. Ashraf, L. Biniek, H. Bronstein, C. Combe, J. E. Donaghy, D. I. James, C. B. Nielsen, B. C. Schroeder, W. Zhang, *Acc. Chem. Res.* 2012, **45**, 714.
- B. C. Schroeder, R. S. Ashraf, S. Thomas, A. J. P. White, L. Biniek, C. B. Nielsen, W. Zhang, Z. Huang, P. S. Tuladhar, S. E. Watkins, T. D. Anthopoulos, J. R. Durrant, I. McCulloch, *Chem. Commun.* 2012, **48**, 7699.
- H. Bronstein, R. S. Ashraf, Y. Kim, A. J. White, T. Anthopoulos, K. Song, D. James, W. Zhang, I. McCulloch, *Macromol. Rapid Commun.* 2011, **32**, 1664.
- H. Bronstein, D. S. Leem, R. Hamilton, P. Woebkenberg, S. King, W. Zhang, R. S. Ashraf, M. Heeney, T. D. Anthopoulos, J. de Mello, I. McCulloch, *Macromolecules* 2011, **44**, 6649.
- Z. Fei, R. S. Ashraf, Z. Huang, J. Smith, R. J. Kline, P. D'Angelo, T. D. Anthopoulos, J. R. Durrant, I. McCulloch, M. Heeney, *Chem. Commun.* 2012, **48**, 2955.
- Q. Zheng, B. J. Jung, J. Sun, H. E. Katz, *J. Am. Chem. Soc.* 2010, **132**, 5394.
- J.-Y. Wang, S. K. Hau, H.-L. Yip, J. A. Davies, K.-S. Chen, Y. Zhang, Y. Sun, A. K.-Y. Jen, *Chem. Mater.* 2011, **23**, 765.

16. J.-S. Wu, Y.-J. Cheng, M. Dubosc, C.-H. Hsieh, C.-Y. Chang, C.-S. Hsu, *Chem. Commun.* 2010, **46**, 3259.
17. Y.-J. Cheng, C.-H. Chen, Y.-S. Lin, C.-Y. Chang, C.-S. Hsu, *Chem. Mater.* 2011, **23**, 5068.
18. Y.-J. Cheng, J.-S. Wu, P.-I. Shih, C.-Y. Chang, P.-C. Jwo, W.-S. Kao, C.-S. Hsu, *Chem. Mater.* 2011, **23**, 2361.
19. C.-Y. Chang, Y.-J. Cheng, S.-H. Hung, J.-S. Wu, W.-S. Kao, C.-H. Lee, C.-S. Hsu, *Adv. Mater.* 2012, **24**, 549.
20. Y.-J. Cheng, S.-W. Cheng, C.-Y. Chang, W.-S. Kao, M.-H. Liao, C.-S. Hsu, *Chem. Commun.* 2012, **48**, 3203.
21. R. S. Ashraf, Z. Chen, D. S. Leem, H. Bronstein, W. Zhang, B. Schroeder, Y. Geerts, J. Smith, S. Watkins, T. D. Anthopoulos, H. Siringhaus, J. C. de Mello, M. Heeney, I. McCulloch, *Chem. Mater.* 2010, **23**, 768.
22. M. Zhang, X. Guo, X. Wang, H. Wang, Y. Li, *Chem. Mater.* 2011, **23**, 4264.
23. W. Li, L. Yang, J. R. Tumbleston, L. Yan, H. Ade, and W. You, *Adv. Mater.* 2014, **26**, 4456.
24. Y.-X. Xu, C.-C. Chueh, H.-L. Yip, F.-Z. Ding, Y.-X. Li, C.-Z. Li, X. Li, W.-C. Chen, and A. K.-Y. Jen, *Adv. Mater.* 2012, **24**, 6356.
25. K. C. Lee, S. Song, J. Lee, D. S. Kim, J. Y. Kim, C. Yang, *Chem. Phys. Chem.*, 2014, DOI: 10.1002/cphc.201402461.
26. C.-Z. Li, C.-C. Chueh, H.-L. Yip, K. M. O'Malley, W.-C. Chen, and A. K.-Y. Jen, *J. Mater. Chem.* 2012, **22**, 8574.
27. K. M. O'Malley, C.-Z. Li, H.-L. Yip, and A. K.-Y. Jen, *Adv. Energy Mater.* 2012, **2**, 82.
28. H. Zhou, L. Yang, A. C. Stuart, S. C. Price, S. Liu, W. You, *Angew. Chem. Int. Ed.* 2011, **50**, 2995.